Available online at www.sciencedirect.com
ScienceDirect
Nuclear Instruments and Methods in Physics Research A 574 (2007) 425–432
NUCLEAR INSTRUMENTS & METHODS IN PHYSICS RESEARCH Section A
www.elsevier.com/locate/nima

Bulk micromegas detectors for large TPC applications

J. Bouchez[a], D.R. Burke[a], Ch. Cavata[a], P. Colas[a], X. De La Broise[a], A. Delbart[a], A. Giganon[a], I. Giomataris[a], P. Graffin[a], J.-Ph. Mols[a], F. Pierre[a], J.-L. Ritou[a], A. Sarrat[a], E. Virique[a], M. Zito[a,*], E. Radicioni[b], R. De Oliveira[c], J. Dumarchez[d], N. Abgrall[e], P. Bene[e], A. Blondel[e], A. Cervera[e,1], D. Ferrere[e], F. Maschiocchi[e], E. Perrin[e], J.-P. Richeux[e], R. Schroeter[e], G. Jover[f], T. Lux[f], A.Y. Rodriguez[f], F. Sanchez[f]

[a] *Dapnia, CEA-Saclay, 91191 Gif-Yvette, France*
[b] *INFN Sezione di Bari, Bari, Italy*
[c] *CERN/TS-DEM, CH 1211 Geneva, Switzerland*
[d] *LPNHE, Université Paris-VI-VII, Paris, France*
[e] *DPNC, Section de Physique, University of Geneva, CH 1211 Geneva 4, Switzerland*
[f] *UAB, IFAE, Bellaterra E-08193, Barcelona, Spain*

Received 11 January 2007; received in revised form 9 February 2007; accepted 11 February 2007
Available online 7 March 2007

Abstract

A large volume TPC will be used in the near future in a variety of experiments including T2K. The bulk Micromegas detector for this TPC is built using a novel production technique particularly suited for compact and robust low mass detectors. The capability to pave a large surface with a simple mounting solution and small dead space between modules is of particular interest for these applications. We have built several large bulk Micromegas detectors ($27\times 26\,\mathrm{cm}^2$) and we have tested them in the former HARP field cage setup with a magnetic field. Cosmic ray data have been acquired in a variety of experimental conditions. Good detector performances and space point resolution have been achieved.

PACS: 29.40.Cs; 29.40.Gx

Keywords: Micromegas; TPC

1. Introduction

A large volume TPC will be used in the near future for a variety of experiments, including T2K, and it is envisaged for a Linear Collider detector. In the case of the T2K experiment [1], a neutrino beam with peak energy around 600 MeV, produced in the JPARC accelerator complex in Tokai (Japan), will be directed towards the SuperKamiokande detector 295 km away. A near detector will be installed at 280 m from the proton target. It will measure the neutrino flux and spectrum and the ν_e contamination of the beam. A detailed program of measurements of various neutrino-nucleus cross-sections is also foreseen.

This magnetized near detector ($B = 0.2\,\mathrm{T}$) comprises three large TPC which will measure the tracks produced by the interactions of the neutrino beam in two plastic scintillator active targets. The requirements on the performances of these TPC, dictated by the physics program of T2K, are: momentum resolution better than 10% at a momentum of $1\,\mathrm{GeV}/c$, and good $\mathrm{d}E/\mathrm{d}x$ measurement, better than 10%, to distinguish the electrons produced by ν_e interactions, from the muons produced by ν_μ interactions. The area to be instrumented corresponds to almost $10\,\mathrm{m}^2$ and a pad size around $70\,\mathrm{mm}^2$ is considered. Of course the pad size depends on the specific application. In our case it has been chosen taking into account several

*Corresponding author. Tel.: +33 1 69083819; fax: +33 1 69086428.
E-mail address: zito@dapnia.cea.fr (M. Zito).
[1] Now at University of Valencia, Spain.

0168-9002/$ - see front matter © 2007 Elsevier B.V. All rights reserved.
doi:10.1016/j.nima.2007.02.074

factors, from physics requirements to readout complexity and cost.

For the TPC readout plane, the 'bulk' Micromegas technology [2] is the best technical solution to minimize the dead zones on the edges of the modules and to improve the gas gain uniformity. Moreover, this technique is suited to industrialization and mass production, thereby offering the perspective of a cheap alternative to wire chambers.

This technique for manufacturing Micromegas detectors in a single process has been developed in 2004 by a CERN-Saclay collaboration and is described in detail in Ref. [2]. A woven mesh is laminated on a Printed Circuit Board (PCB) covered by a photoimageable film. At the end of the process, the micromesh is sandwiched between two layers of insulating material. The detector undergoes then UV exposure with an appropriate mask, followed by chemical development. A few millimeter wide border at the edge can thus be produced and avoids the need of an external additional frame to support the stretched micromesh. Such a detector 'all-in one', called 'bulk' Micromegas, is robust and allows large areas, up to $50 \times 50\,\mathrm{cm}^2$ or more, to be made in one piece.

In the following section we describe the detectors that we have designed and built. Section 3 documents the experimental setup for the TPC tests at CERN. The results of these tests are reported in Section 4.

2. The bulk Micromegas detector

One end plate for the T2K TPC has dimensions of approximately $0.7 \times 2\,\mathrm{m}^2$. In our design, this large surface, which is also typical for other applications, is segmented with detector units of area around $30 \times 30\,\mathrm{cm}^2$ that can be easily replaced. In particular, no service or connection is needed from the inner volume of the TPC.

Following these design considerations, four bulk Micromegas detectors have been built in the CERN/TS-DEM PCB production facility. The PCB, segmented into 1020 pads, $8 \times 8\,\mathrm{mm}^2$, with a $100\,\mu\mathrm{m}$ insulation between them (Fig. 1) is 3 mm thick. It comprises two layers of FR4 with blind vias in the inner layer (Fig. 2). This solution avoids the gas tightness problems arising from the conventional two layers structure with vias sealed with epoxide resins. The top conductive layer is realized with $20\,\mu\mathrm{m}$ thick copper deposited on FR4.

The pads are arranged in 32 rows of 32 pads for an active surface of $26.76 \times 26.35\,\mathrm{cm}^2$. In one corner a four pad equivalent surface is reserved for the Micromesh high voltage supply connection from the backside of the PCB. A half-pad staggering from one row to the next assures a more uniform track reconstruction performance for high momentum vertical tracks. For a track whose projection in the readout plane corresponds to the center of one pad, practically all the primary electrons will be collected by this pad, thereby giving a space point of limited precision. However, thanks to the staggering, the projection of the same track will be at the border between two pads in the following row, resulting in a space point of much higher precision.

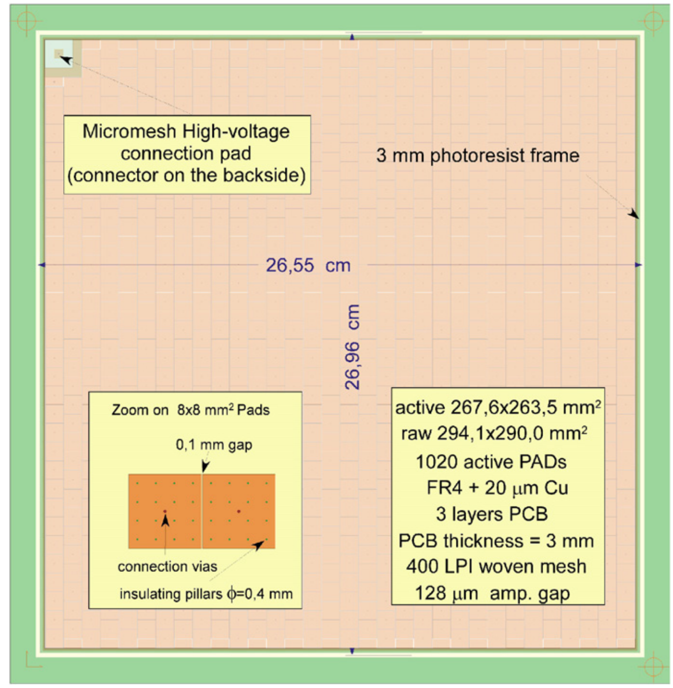

Fig. 1. View of the PCB from the anode pads side.

A sandwich of two layers of $64\,\mu\mathrm{m}$ Pyralux PC1025 Photoimageable coverlay by DuPont [4], a woven micromesh and finally a layer of Pyralux is laminated on the PCB. The woven micromesh [3], is built out of $19\,\mu\mathrm{m}$ thick 304L stainless steel wires. After weaving its thickness is reduced by 20–30% by a lamination process. The wires are spaced with a pitch of $59\,\mu\mathrm{m}$. After photo-imaging, the mesh is held in place by the coverlay frame and 16 320 regularly distributed 0.4 mm diameter cylindrical pillars, maintaining the amplification gap of $128\,\mu\mathrm{m}$.

After protecting the sensitive detector surface with a melamine plate, the outer coverlay and PCB frame is cut to 3 mm in order to reduce the inactive area. Finally, the detector is glued onto an Aluminum support structure (Fig. 3) to reinforce the PCB mechanical rigidity and to assure a 0.1 mm planarity tolerance. This structure hosts the seal for gas tightness.

After the production, the detectors have been tested, first in air and then in a gas box. A good quality detector must stand in air a high voltage of 750 V drawing a current of a few nA. During this process, some defective pads (a few per mille) were identified by measuring the current drawn after grounding each individual pad. These pads, drawing a current larger than 100 nA at a mesh high voltage of 600 V, had to be disconnected.

A gas box provided an easy way to test the detector in a specific gas mixture with a ^{55}Fe source. The box was provided with a mylar window and an electrode to create a drift electric field pushing electrons toward the Micromegas mesh. The energy resolution was measured to be 11% for a

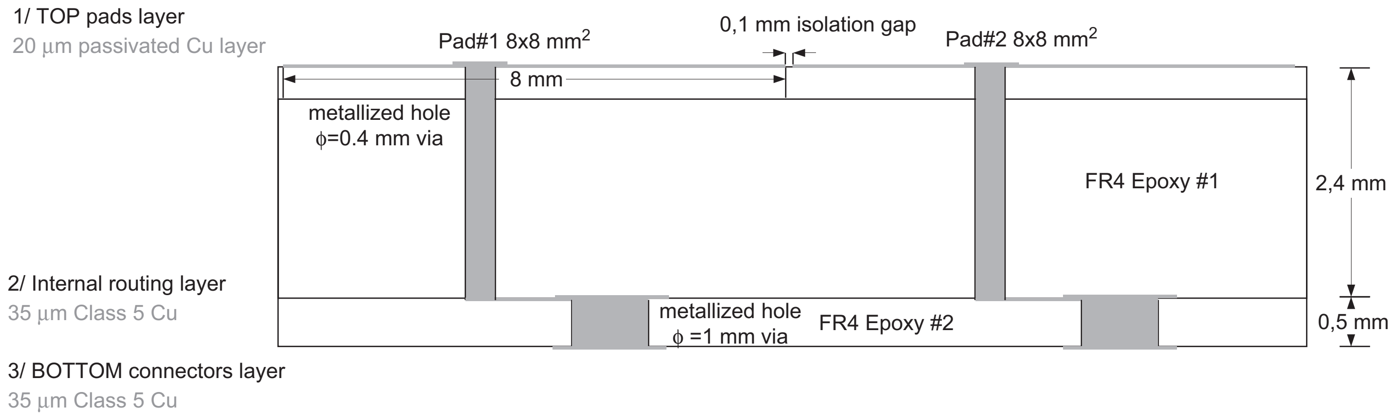

Fig. 2. The PCB cross-section.

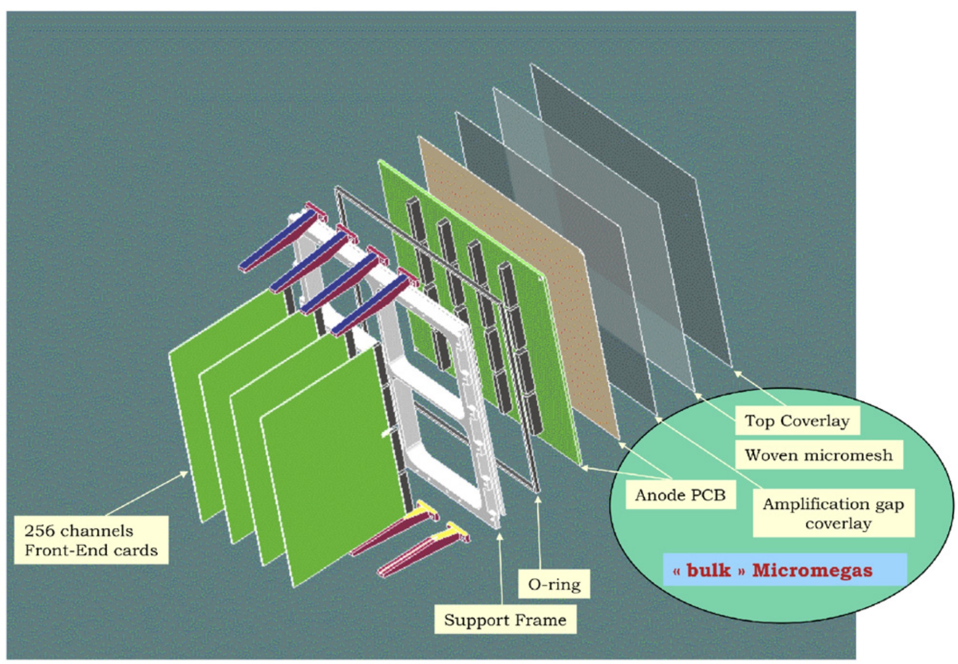

Fig. 3. Exploded 3D view of a Micromegas module.

5.9 KeV X-ray from the width of the Fe line (Fig. 4). Several gas mixtures were tested with maximum gains ranging from a few thousand ($Ar-CO_2$, $Ar-CF_4$) to a few 10^4 in $Ar-CF_4-iC_4H_{10}$. For the latter mixture, the small Isobutane fraction, below the flammability limit, provides the required stability of operation while keeping all the interesting properties of an $Ar-CF_4$ mixture: large drift velocity, low diffusion coefficient even in low magnetic field and long lifetime of the drifting electrons.

3. The TPC experimental setup

The TPC experimental setup at CERN consists of the former HARP TPC field cage inside a solenoidal magnet and its gas system, read out by the Alice TPC 10 MHz electronics. The TPC field cage is described in more detail in Ref. [5]. It consists of a large cylindrical vessel, 80 cm inner diameter and 154.1 cm in drift length, where a series of strips connected by a resistor chain creates an axial electric field. The cathode was set at a potential corresponding to an electric field of 160 V/cm. The TPC field cage is mounted inside a solenoidal magnet of 90 cm inner diameter and 225 cm length.

The end-plate hosting two Micromegas modules (Fig. 5) consists of an aluminum support structure covered on its inner surface by a large PCB with copper coating for an uniform termination of the drift electric field. The total inactive region between the two Micromegas sensitive regions is 12 mm.

The tests have been performed with the gas mixture $Ar-CF_4(3\%)-iC_4H_{10}(2\%)$. It offers a fairly large drift velocity (6.5 cm/µs) close to its maximum at the electric

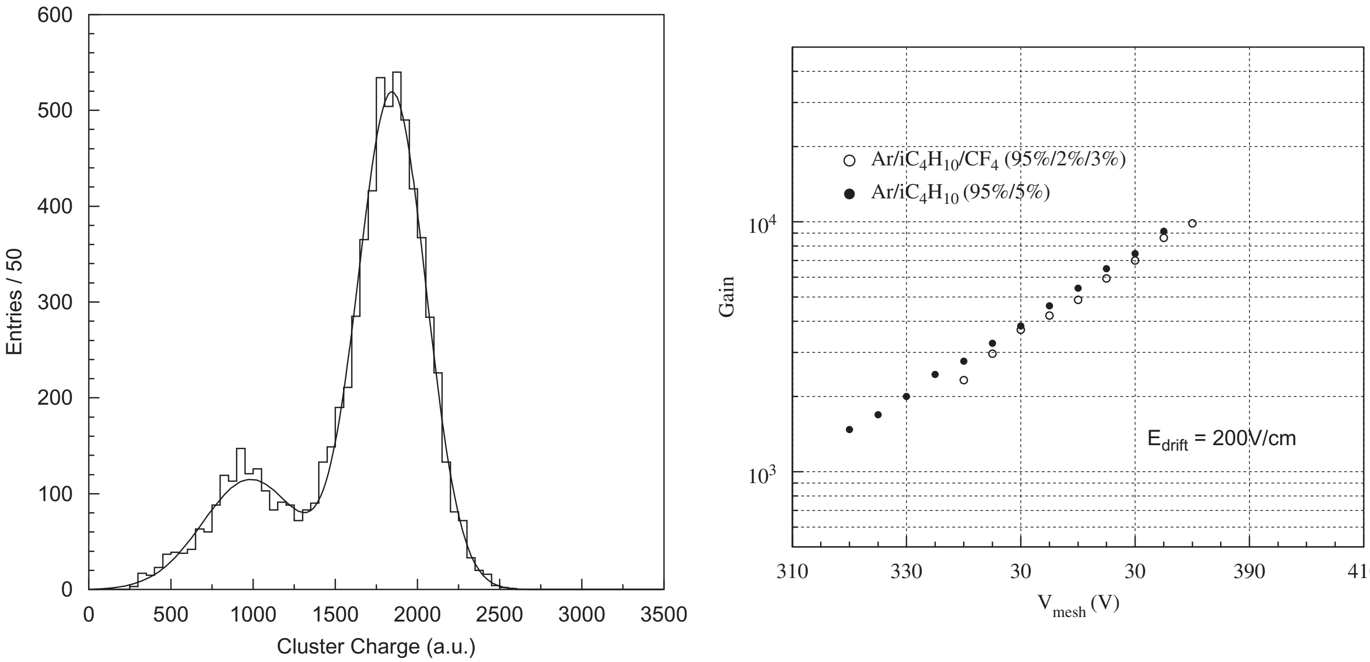

Fig. 4. Left: charge spectrum obtained with a Fe55 X-ray source showing a resolution of 11%. Right: gain versus micromesh high voltage in $Ar-iC_4H_{10}(5\%)$ (black dots) and $Ar-CF_4(3\%)-iC_4H_{10}(2\%)$ (open circles).

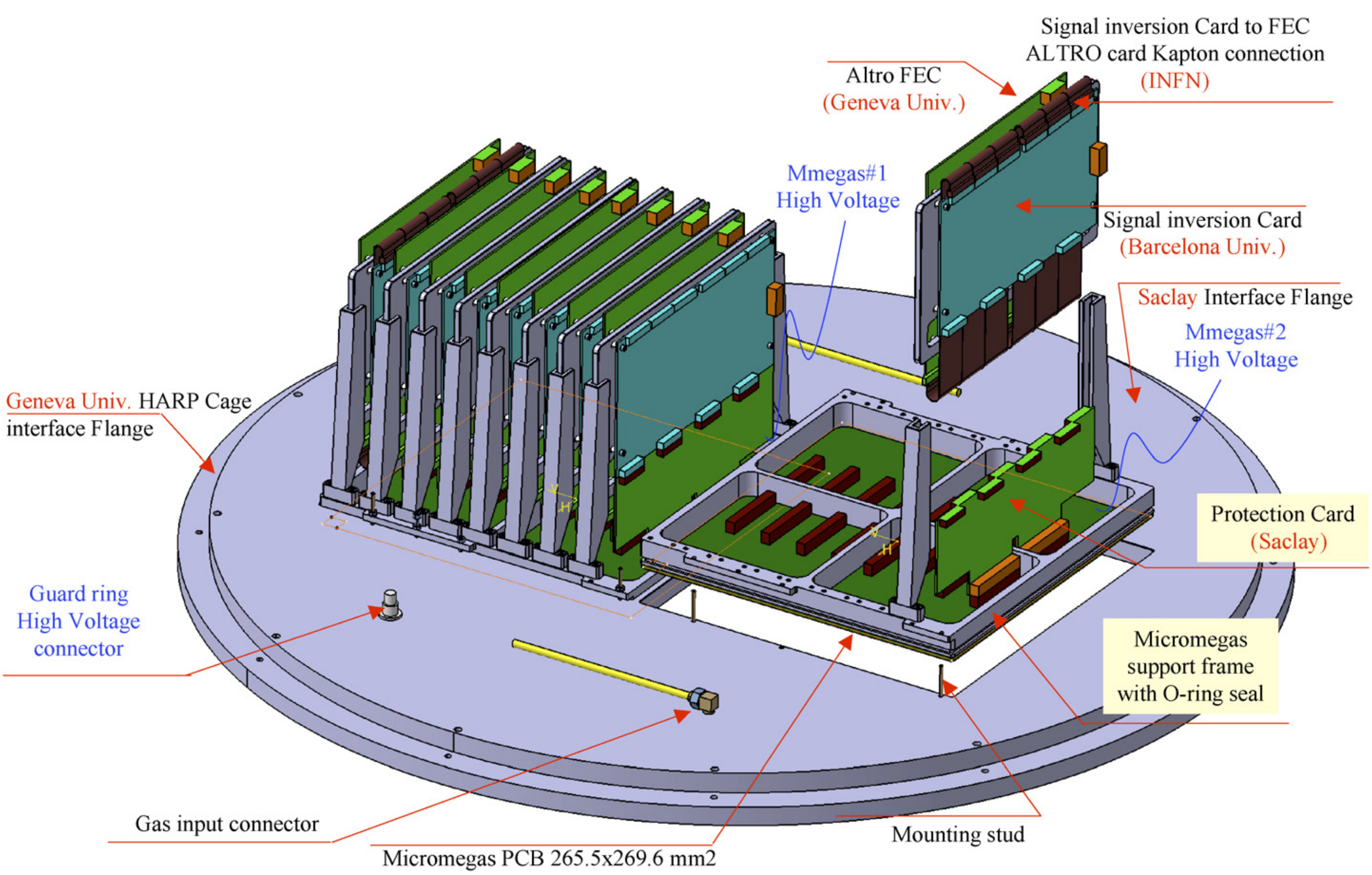

Fig. 5. The TPC endplate with two Micromegas detectors and the readout electronics.

field of 160 V/cm, low diffusion coefficient at small magnetic field ($237\,\mu\mathrm{m}/\sqrt{\mathrm{cm}}$ for $B = 0.2\,\mathrm{T}$) and allows operation of Micromegas with a gain up to 10^4 and more.

A system of seven scintillators, above and below the magnet, equipped with PMT, provided the trigger signal. The electronics consists of 12 invertor boards and 12 Alice TPC Front End Cards cards [6] for a total of 1536 channels. The invertor boards were necessary to adapt the polarity of the signal from Micromegas pads to the Alice Front End Cards. The cards instrumented the central part of the active region of the two detectors, for a total vertical length of 38.4 cm over 48 rows of pads. The input noise level was 2000 e RMS for a sampling frequency of 10 MHz, a shaping time of 190 ns and a charge to ADC conversion factor of 1000 e per ADC count.

4. Results

We have taken cosmic ray data with this setup with the $Ar-CF_4(3\%)-iC_4H_{10}(2\%)$ gas mixture for almost one month. Typical Micromegas voltages were 330–360 V corresponding to gains between 2000 and 10 000. The magnetic field varied from 0 to 0.4 T. The detector operated smoothly, the typical current drawn from the power supply being 1 nA. We observed sporadic sparks, triggering the current limit of the detector high voltage power supply (500 nA), without consequence neither for the detector nor for the electronics.

Data taken with cosmic rays have been analyzed using a complete analysis chain including an event display, a reconstruction program and a full simulation based on the Geant4 package [7]. A threshold equal to 3.5 times the RMS of the pedestal (typically two ADC counts) is applied to the raw data.

Hits on pads in the same row are associated in a cluster. In the case of clusters with two pads, the position cannot be estimated using a simple barycenter as the pad width is much larger than the electron cloud size, introducing large non-linearities. If the charge $q(q)'$ has been collected on the pad extending from x_p to $x_p + \Delta_p$ ($x_p - \Delta_p$ to x_p), then

$$\frac{q}{q+q'} = \frac{\int_{x_p}^{x_p+\Delta_p} G(u, x_t, w_t)\,\mathrm{d}u}{\int_{x_p}^{x_p+\Delta_p} G(u, x_t, w_t)\,\mathrm{d}u + \int_{x_p-\Delta_p}^{x_p} G(u, x_t, w_t)\,\mathrm{d}u} \tag{1}$$

where $G(x, x_t, w_t) = (1/\sqrt{2\pi}w_t)\mathrm{e}^{-(x-x_t)^2/2w_t^2}$ represents the probability density function of the primary electron cloud reaching the pad, neglecting the angle of the track with respect to the normal to the measured coordinate x. The Gaussian width w_t is estimated from $w_t = C_t\sqrt{l_d}$, where C_t is the transverse diffusion coefficient computed using the Magboltz program [8] and l_d is the drift length. Using numerical methods we solve Eq. (1) and find the best estimate of the track coordinate x_t.

The uncertainty σ_x (Fig. 6) of the track coordinate x_t is estimated in the limit $\Delta_p/w_t \gg 1$ taking into account the binomial fluctuations of the number of primary electrons collected by the two pads [9]:

$$\sigma_x = \sqrt{2\pi}w_t\mathrm{e}^{(x_t-x_p)^2/2w_t^2}\sqrt{\frac{f(1-f)}{\alpha N_p}} \tag{2}$$

where $f = q/(q+q')$, N_p is the number of primary electrons in the cloud estimated from the total collected charge $(q+q')$ and $\alpha \simeq 0.5$ is a reduction factor to take into account gain fluctuations. Indeed gain fluctuations due to the stochastic nature of the avalanche process reduce the number of effective primary electrons to be considered in the uncertainty evaluation. The pull distribution (Fig. 6) of

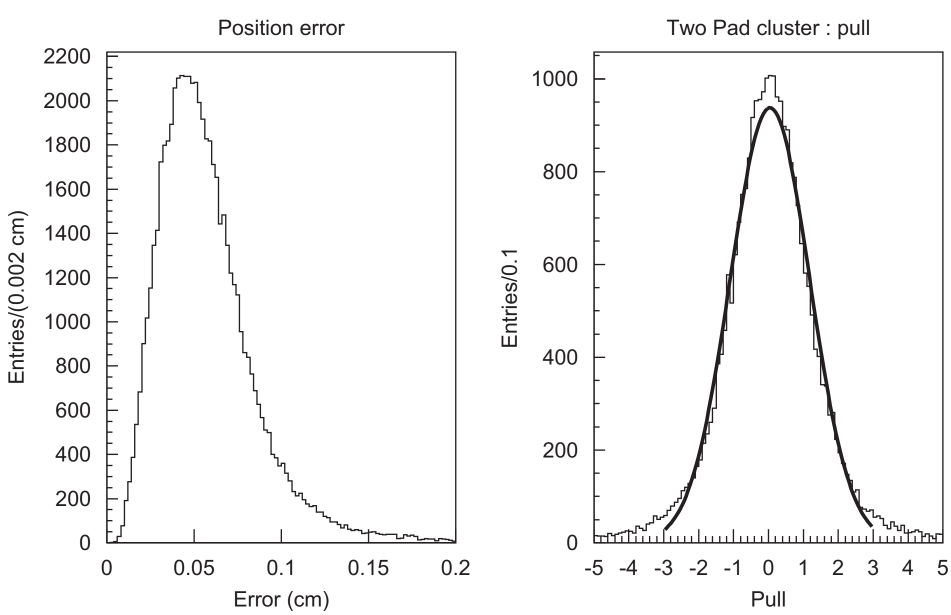

Fig. 6. Left plot: the estimated error distribution associated to clusters with two pads for $B = 0.2\,\mathrm{T}$. The mean value of the distribution is 570 μm. Right plot: the pull of the cluster position with respect to the fit position of the track. The curve represents a Gaussian fit to the distribution with a width of 1.1.

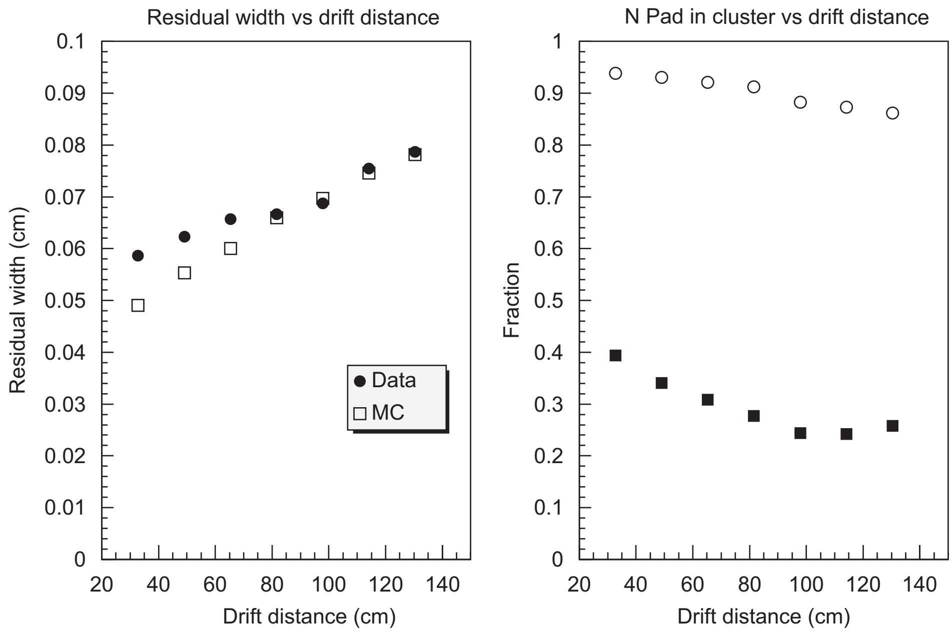

Fig. 7. Left plot: the Gaussian width for the two pad cluster track residual as a function of the drift distance for $B = 0.2\,\mathrm{T}$. The open squares show the width estimated using a Geant4 MC simulation. Right plot: the cumulative fraction of clusters with one pad (squares) and two pads (open circles).

the cluster position with respect to the fit position of the track has a width of approximately 1 assuming that the number of effective electrons is one half of the electrons in the cloud. This reduction factor is in fair agreement with expectations from numerical simulations [10]. A term representing the electronic noise affecting the measurement of the charges q and q' is added in quadrature to the right-hand side of Eq. (2).

For clusters with three hits, the position is estimated in a similar way, fitting a Gaussian distribution to the two measured charge ratios. We have associated an uncertainty equal to $\Delta_p/\sqrt{12}$ to clusters with only one hit, where Δ_p is the pad width.

Tracks close to the vertical axis and crossing the two Micromegas modules are reconstructed and fitted separately in the two projections (one in the readout plane, the other in the plane containing the vertical axis and the drift direction) with a least square fit. The space point resolution for each cluster has been studied considering the residual between its position and the extrapolated track position without using this clusters. Fig. 7 shows the Gaussian widths of these residuals for $B = 0.2\,\mathrm{T}$ in fair agreement with the result of the Geant4 simulation. To estimate the momentum resolution capabilities of this device it is necessary to consider the fraction of rows with one, two or more pad hit (Fig. 7): approximately 75% of the clusters have two or more hits at one meter drift length for $B = 0.2\,\mathrm{T}$. This is the experimental situation corresponding to the T2K TPC. The momentum resolution of a TPC equipped with these detectors and measuring a track length of 70 cm in a 0.2 T magnetic field is expected to be 8% at $1\,\mathrm{GeV}/c$, slightly better than the required performance of 10% for the T2K tracker.

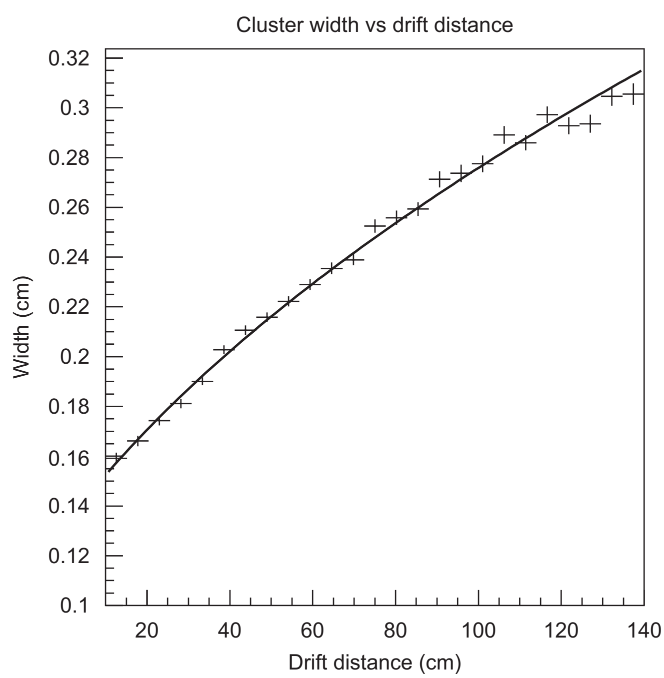

Fig. 8. Gaussian width of the electron cloud measured using the track position and the charge ratio in clusters with two pads as a function of the drift distance for $B = 0.2\,\mathrm{T}$. The curve shows the result of the fit to the function $\sqrt{s_0^2 + C_\mathrm{T}^2 l_\mathrm{drift}}$ where the transverse diffusion coefficient C_T has been found $253\,\mu\mathrm{m}/\sqrt{\mathrm{cm}}$.

A first study of the gas properties has been done during the data taking by studying tracks that cross the field cage cathode. These tracks give a very precise measurement of the drift velocity that is in agreement with the Magboltz predictions. Clusters with two pads can be used to study the width of the electron cloud if the position given by the track fit is assumed. Starting from Eq. (1), we solve this time for w_t. From the track parameters fit on all measured points, we compute x_t as the extrapolation of the track to the pad. The result is shown in Fig. 8. The mean value of the distribution of w_t as a function of the drift length l_d has been fit with the function $\sqrt{s_0^2 + C_T^2 l_d}$. The first term models the uncertainty due to the track position. The values for the transverse diffusion coefficient C_T are in reasonable agreement with the Magboltz predictions (Table 1). The attenuation in the Ar$-CF_4$–Isobutane mixture was found to be negligible after a few days of gas flow with a lower limit on the attenuation length of 30 m.

A first study of the measurement of dE/dx, the energy loss per unit length, has been performed considering for each track the total charge detected in each pad row. A truncated mean retaining only 80% samples with lower measured charge has been used. This mean has been corrected for the track length in the active volume of the TPC. The results are shown in Fig. 9. A resolution on the dE/dx of $12.2 \pm 0.4\%$ (Fig. 9) has been obtained for a nominal track length of 38.4 cm and 48 samples. Using the PDG parametrization [11], a resolution around 10% is expected for this track length. The T2K requirement on the dE/dx will be met using these detectors: indeed in T2K the track length will be of 70 cm for 72 samples. The expected dE/dx resolution will be below 10%.

Table 1
Expected (Magboltz predictions) and measured (last two columns) gas properties (drift velocity v_d (cm/μs) and transverse diffusion coefficient C_T (μm/$\sqrt{\text{cm}}$)) for different experimental conditions

Mag. Field (T)	El. Field (V/cm)	v_d (exp)	C_T (exp)	v_d (meas)	C_T (meas)
0	160	6.50	309	6.26 ± 0.05	302 ± 15
0.2	160	6.50	237	6.27 ± 0.05	253 ± 15
0.4	160	6.50	157	6.30 ± 0.05	173 ± 15
0.4	100	4.46	157	4.23 ± 0.02	176 ± 15

5. Conclusion

We have built four large bulk Micromegas detectors as prototypes for the T2K TPC. We have tested these detectors in the former HARP field cage setup with a magnetic field. Cosmic ray data have been acquired in a variety of experimental conditions. The detector has shown good performances in terms of gain and space point resolution.

To validate that this space point resolution meets the requirements set by the T2K physics program, we have used the Gluckstern formula [11] for the momentum resolution. We assume a space point resolution of 700 μm at 1 m drift distance, and consider that only 75% of the rows will contribute to this measurement (cluster with one pad hit have a poor resolution). In the T2K TPC, there will be 72 samples on a track length of 70 cm. We obtain a momentum resolution of 8.3% at a momentum of 1 GeV which satisfy the requirement described in Section 1. Further improvements are expected because of the lower noise of the TPC final electronics. This will allow to set a lower threshold and therefore to use a larger fraction of the space points.

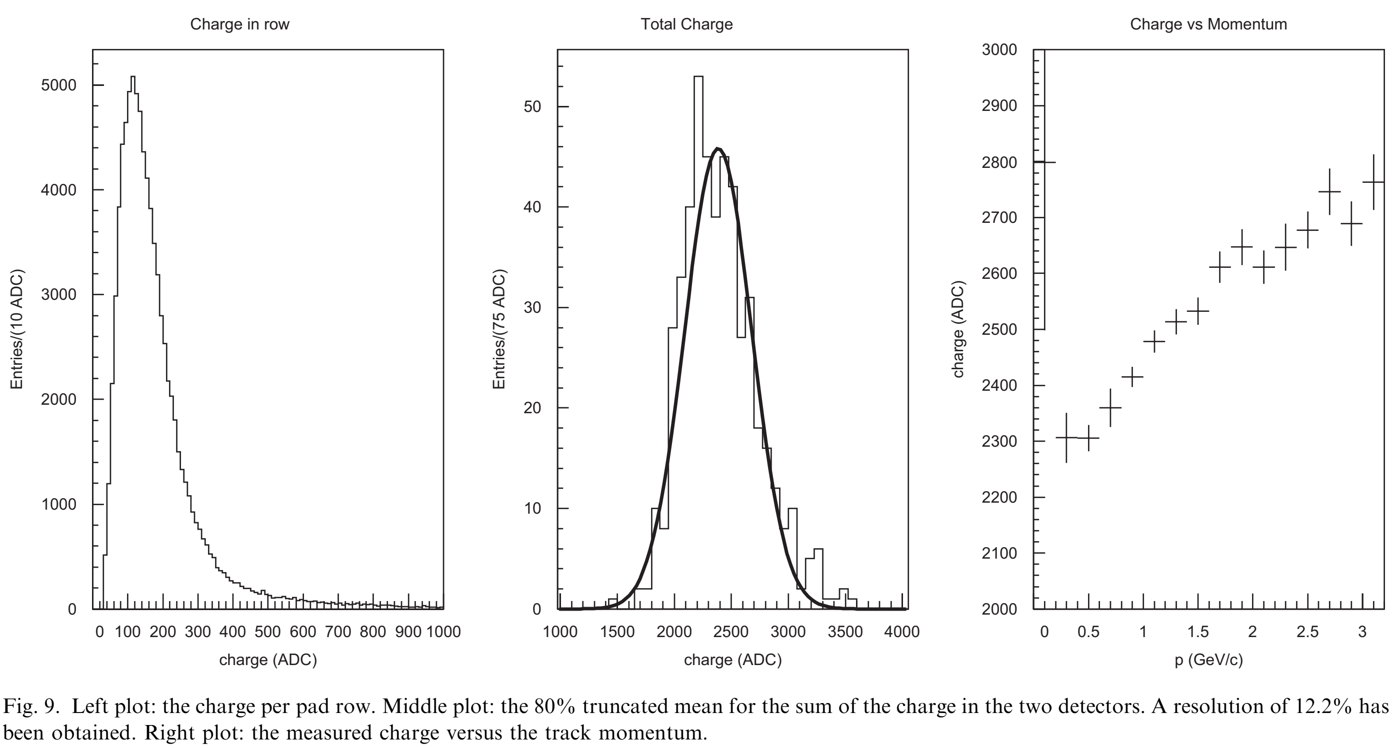

Fig. 9. Left plot: the charge per pad row. Middle plot: the 80% truncated mean for the sum of the charge in the two detectors. A resolution of 12.2% has been obtained. Right plot: the measured charge versus the track momentum.

Acknowledgments

We wish to warmly thank Luciano Musa for his kind assistance in setting up and operating the electronic chain and the DAQ software.

References

[1] Y. Itow, et al., hep-ex/0106019.
[2] I. Giomataris, et al., Nucl. Instr. and Meth. A 560 (2006) 405.
[3] Gantois, B.P. 307, F-88105 Saint Die des Vosges cedex, France.
[4] DuPont Electronic Materials, 14 Alexander Drive—Research Triangle Park, NC 27709-4425.
[5] G. Prior, Nucl. Phys. B Proc. Suppl. 125 (2003) 37.
[6] L. Musa, et al., Proceedings of the IEEE Nuclear Science Symposium, Portland, 2003 ⟨http://ep-ed-alice-tpc.web.cern.ch⟩.
[7] S. Agostinelli, et al., Nucl. Instr. and Meth. A 506 (2003) 250.
[8] S. Biagi, Nucl. Instr. and Meth. A 421 (1999) 234.
[9] D. Karlen, et al., Nucl. Instr. and Meth. A 555 (2005) 80 (Appendix A).
[10] M. Kobayashi, Nucl. Instr. and Meth. A 562 (2006) 136.
[11] W.M. Yao, et al., J. Phys. G 33 (2006) 1.